6533

Optical Properties of Dye Molecules Adsorbed on Single Gold and Silver Nanoparticles

Stefan Franzen,* Jacob C. W. Folmer, Wilhelm R. Glomm, and Ryan O'Neal

Department of Chemistry, North Carolina State University, Raleigh, North Carolina 27695

Received: January 20, 2002; In Final Form: April 19, 2002

Despite the well-known relationship between the resonance Raman excitation profile and the absorption line shape, there is scant experimental evidence for effects in absorption or fluorescence spectroscopy related to the observations of surface-enhanced Raman scattering (SERS). On the other hand, numerous Raman studies have been done on the SERS phenomenon, where large enhancement factors have been determined. In this work, the absorption properties of molecules adsorbed on single gold and silver nanoparticles (monomers) have been investigated, with particular emphasis on an examination of the effect on the spectrum of the adsorbate. A number of the adsorbates studied are similar to those reported in SERS studies. The adsorbates can be divided into two classes according to the nature of the interaction with the adsorbent. Class I shows little change in the absorption spectrum. Class II shows a large reduction in absorption. The only examples of an increase in absorption arise from solvatochromic effects. The implication of these observations for the mechanism of SERS is discussed.

Introduction

Since its discovery in 1974, the mechanism for surface enhanced Raman scattering (SERS) has been a matter of considerable debate.[1-10] It has been widely accepted that there are two mechanisms for the observed, and at times huge, enhancement factors in SERS: the electromagnetic (EM) and the chemical mechanism. The EM mechanism is based on the interaction of the electric field of surface plasmons with the transition moment of an adsorbed molecule, whereas the chemical mechanism is based on the idea that mixing of molecular and metal states can occur. Although the two are not necessarily mutually exclusive, the use of roughened geometries such as island films,[11-20] roughened electrodes,[3,21] encapsulated particles,[22-25] and particularly aggregated nanoparticle clusters[6,9,26-40] have tended to substantiate that the EM mechanism is the essential one,[41] to which the chemical effect may or may not provide additional enhancement.

Although a large number of theories have appeared to explain the existence of the SERS phenomenon, the majority of these theories tend to ignore the implications for other optical properties such as absorption and emission. A theoretical treatment has shown that the theoretical maximum enhancement in the absorption spectra of Rhodamine B adsorbed to silver is expected to be approximately 50 for ellipsoidal particles, whereas for spherical silver nanoparticles it is expected to be smaller.[42] On the other hand, the calculated values for Raman enhancement (SERS) factors of up several thousand reported for nanoparticle samples are consistent with observations in colloidal solutions.[28,37,43] The enhancements reported in colloidal suspensions are vastly smaller than the enhancements reported in recent work based on single molecule detection.[44-46] Given the number of conflicting reports and theories, it is indeed useful to consider optical techniques other than Raman spectroscopy that can provide complementary information about the system and the nature of the enhancement.

The EM mechanism is based on the hypothesis that the superposition of the incident and scattered fields interacts with the transition moment of a molecule near the surface.[1,7] Surface selection rules determine the polarization required for enhancement. Local field effects near the surface of a conducting sphere provide a means for amplification of EM fields near the surface. Since the Raman cross section depends on the fourth power of the transition moment, an amplification of the electric field can, in principle, increase scattering by a relatively large factor. In the time-correlator formalism, the resonance Raman scattering cross section, σ_R can be expressed as[47]

$$\sigma_R = \frac{8\pi\omega_s^3\omega_0 M_{if}^4}{9\hbar^2 c^4}\left(\int_0^\infty \langle f|i(t)\rangle \exp\{i(\omega_i + \omega_0)t - \Gamma t\}\,dt\right)^2 \tag{1}$$

In this expression, M_{if} is the transition moment of the molecule, ω_0 is the frequency of incident radiation, ω_s is the frequency of scattered radiation, ω_i is the vibrational frequency in the ground state, and Γ is the damping constant. The absorption cross section, σ_A, is related to the resonance Raman cross section as indicated in eq 2,[47]

$$\sigma_A = \frac{2\pi\omega_0 M_{if}^2}{3\hbar c}\int_{-\infty}^\infty \langle i|i(t)\rangle \exp\{i(\omega_i + \omega_0)t - \Gamma t\}\,dt \tag{2}$$

Although the absorption line shape and Raman excitation profile differ because of the difference in their correlation functions the prefactors depend on M_{if}^2 and M_{if}^4, respectively. Despite this well-known difference in the dependence on transition moment, the probability of both processes, absorption and resonant Raman, depends linearly on the intensity of incident radiation and in turn on the square of the incident radiation field. The intensity I equals $1/2\epsilon_0 c E_0^2$, where E_0 is the electric field amplitude of incident radiation. Enhancements of the local electric field, E_0, will lead to an increase in the transition probability, as widely discussed in studies of SERS.[6,44,45,48] For a spherical metal nanoparticle (herein referred to as a monomer)

* To whom correspondence should be addressed. E-mail: Stefan_Franzen@ ncsu.edu. Phone: (919)-515-8915. Fax: (919)-515-8909.

it has been shown that the tangential and radial fields are as follows:[5]

$$E_t^2 \propto 2E_o^2[1 - g]^2 \qquad (3)$$

$$E_r^2 \propto 2E_o^2[1 + g]^2 \qquad (4)$$

$$g = (\epsilon - \epsilon_o)/(\epsilon + 2\epsilon_o) \qquad (5)$$

where g is a factor related to the polarizability of a metal sphere with a dielectric function, ϵ, in a medium with dielectric constant, ϵ_o. Near the surface plasmon resonance maximum, ϵ approaches $-2\epsilon_o$ and g becomes very large providing a resonance condition.[49] In the case of SERS both the incident and scattered waves can experience the enhancement of the local plasmon field and the overall enhancement can vary as $4E_o^4[1 + g]^4$ for the radial field and $2E_o^4[1 - g]^4$ for the tangential field. This field enhancement implies that the enhancement of absorption or emission intensity should be the square root of the enhancement in the Raman scattering intensity.

Particle dimension and geometry play a large role in determining the enhancement factor in plasmon resonance spectroscopy. This has mainly to do with the coupling of electromagnetic radiation into the electronic structure of the metal. In the case of an elliptical particle, the resonances shift in frequency and potentially lead to larger local fields at the greatest radius of curvature. Aggregates are known to have a strong effect on SERS as well, in part because rough or fractal surfaces can give rise to a stronger coupling of the electric field. A spherical monomer can be viewed as the smallest entity capable of enhancement.[9] Starting with the smallest particles that have a surface plasmon resonance band (3−5 nm), monomers can be viewed as the building blocks for more complex structures with possible surface roughness that can give a specific large enhancement.

It is surprising that despite the well-known relationship between the resonance Raman excitation profile and the absorption line shape, there is scant experimental evidence for enhancement effects in absorption or fluorescence spectroscopy related to the observations of SERS.[50−52] Surface-enhanced infrared effects have been studied for the classic probe molecule *p*-nitrobenzoic acid.[40,53,54] Optical studies on absorption and luminescence by dye-coated silver island films considered the electromagnetic mechanism for coupling between an adsorbate (dye molecule) and adsorbent (metal nanoparticle or surface).[42] Most studies have included the optical properties of both single particles (monomers) and more complicated nanometer-sized metallic structures.[55] Shifts in the plasmon band and large emission as a function of the length and aspect ratio have been reported.[50,56−58]

To improve our understanding of the effect of surface plasmons on absorption and emission, we have studied the absorption spectra of various molecules adsorbed onto monomeric gold and silver nanoparticles with diameters between 5 and 30 nm. The study is intended to examine the effect of adsorbate−particle interactions on the absorption intensity. The study of the spectra of adsorbates similar to those studied by SERS[11,13,21,32,45,46] on spherical monomers represents the first step toward a systematic comparison of the effect of surface plasmons on the absorption spectrum of molecules. We recognize that the experimentally observed transmitted optical intensity is reduced by extinction, i.e., both absorption and scattering. Although scattering is a relatively small contribution

TABLE 1: Adsorbates Used and Their Solvent and Nanoparticle Conditions Attempted[a]

molecule	solvent	nanoparticle	ϵ(M^{-1} cm^{-1})	ω_{max} (cm^{-1})	class
ICG	1, 2	B, C	2.4E+05	12 760	II
CB	2	A, B, C, D	1.4E+05	14 180	II
CV	1, 2	A, B, C	3.9E+04	15 720	II
MG	1, 2	A, B, C, D, E	2.0E+04	15 770	II
MGITC	2	A, B, C, D	7.4E+04	16 200	I/II
RBITC	1, 2	A, B, C, D, E	4.5E+04	18 080	I
E5ITC	2	B, C	8.0E+04	19 050	I
F5ITC	2	A, B, C, D	2.5E+04	20 020	I
1PITC	2	B, C	2.5E+04	29 240	I
Pyr	1	A, B	3.1E+03	38 020	I

[a] Solvent conditions are as follows: 1 = d/d water only, 2 = 50:50 mixture of water and methanol. Nanoparticle conditions are as follows: A = BSPP stabilized 10 nm Au nanoparticles, B = citrate stabilized 10 nm Au nanoparticles, C = citrate stabilized 30 nm Au nanoparticles, D = mercaptooctanoate stabilized 10 nm Au nanoparticles, E = citrate stabilized 30 nm Ag nanoparticles. The reported ϵ and ω_{max} values of the lowest energy band for each compound are reported. Except for pyridine these are experimental values determined in the mixed solvent systems and may deviate from literature values due to solvatochromic effects. See text for the definition of class designations.

to the extinction of the relatively small particles utilized here, a baseline offset due to a *change* in scattering is observed in some of the data. Moreover, the change in reflectivity above the plasmon band plays an important role in the observed spectra. By studying monomer spectra, we can obtain information relevant to the *g*-factor enhancement hypothesis on particles with a nearly spherical geometry.

Experimental Section

Crystal violet (CV), methyl green (MG), 1,1′-diethyl-2,2′-dicarbocyanine iodide (CB), indocyanine green (ICG), rhodamine B isothiocyanate (RBI), pyridine (Pyr), and HPLC grade methanol were purchased from Aldrich. Eosin 5-isothiocyanate (E5ITC), 1-pyrene isothiocyanate (1PITC), and malachite green isothiocyanate (MGITC) were purchased from Molecular Probes. Citrate-stabilized gold nanoparticles with diameters of 10, 30, 60, and 100 nm (Ted Pella, Inc.) were studied. More stable preparations of gold nanoparticles were obtained by replacement of citrate by (a) bis(*p*-sulfonatophenyl)triphenylphosphine (BSPP), and (b) HS(CH$_2$)$_7$COOH (mercaptooctanoic acid). Following exchange in solution, excess BSPP was removed by a series of precipitations with salt and methanol followed by removal of the supernate and resuspension of the gold in d/d H$_2$O. A similar procedure was carried out after exchange for the mercaptooctanoate-stabilized nanoparticles. Concentration of the gold sol was determined by the absorption at ω_p = 19 200 cm^{-1} (521 nm) for 10 nm Au and ω_p = 19 100 cm^{-1} (523 nm) for 30 nm Au. Ag (30 nm) nanoparticles were prepared by standard citrate reduction[35] and characterized by TEM. Stock adsorbate solutions were prepared in methanol and dilutions were made with either pure d/d water or a 50/50 vol % water−methanol mixture for a final concentration in sample ranging from 10^{-4} to 10^{-7}M; however preferential treatment was given to concentrations approaching the limit of detection. The adsorbates and their respective solvent conditions tested are given in Table 1. Structures for the dyes used in this study are reported in the Supporting Information.

All absorption measurements were made on a Hewlett-Packard 8453 Chemstation photodiode array spectrophotometer with attached Chemstation software using 0.5 cm cuvettes. Centrifugations were made with a Fisher Scientific Micro 14 tabletop microcentrifuge.
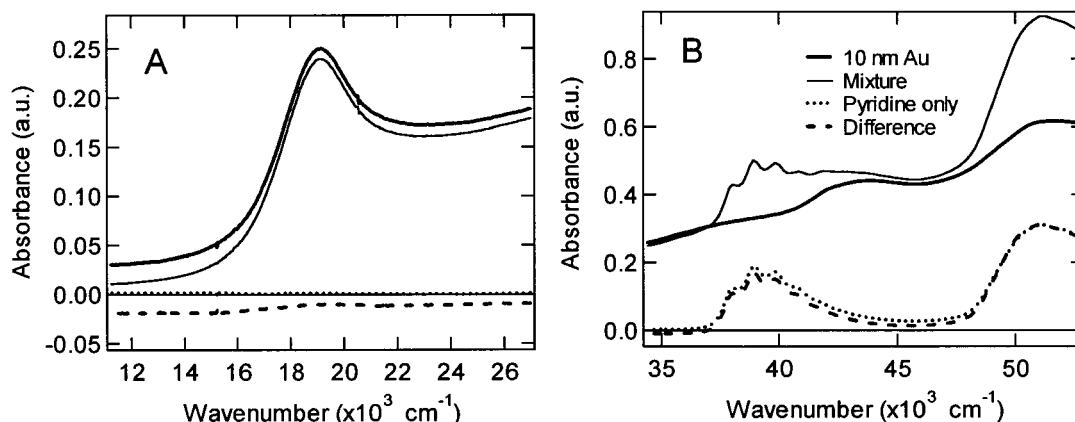
Optical Properties of Dye Molecules

J. Phys. Chem. A, Vol. 106, No. 28, 2002 **6535**

Figure 1. UV−vis spectrum of the class I adsorbate, pyridine (6.7×10^{-5} M), adsorbed to 10 nm BSPP stabilized Au nanoparticles in a 50/50 H$_2$O/MeOH solvent. (A) The plasmon band of 10 nm gold is observed at $\omega_p \approx 19\,200$ cm^{-1}. (B) The pyridine bands at 38 020 and 51 000 cm^{-1} are shown. The bands from the BSPP stabilizer observed at 43 800 cm^{-1} are shown as well in the 10 nm Au spectrum (thick line) and mixture (thin line). These bands are subtracted out in the difference spectrum (---) and compared to free pyridine in solution at the same concentration (···).
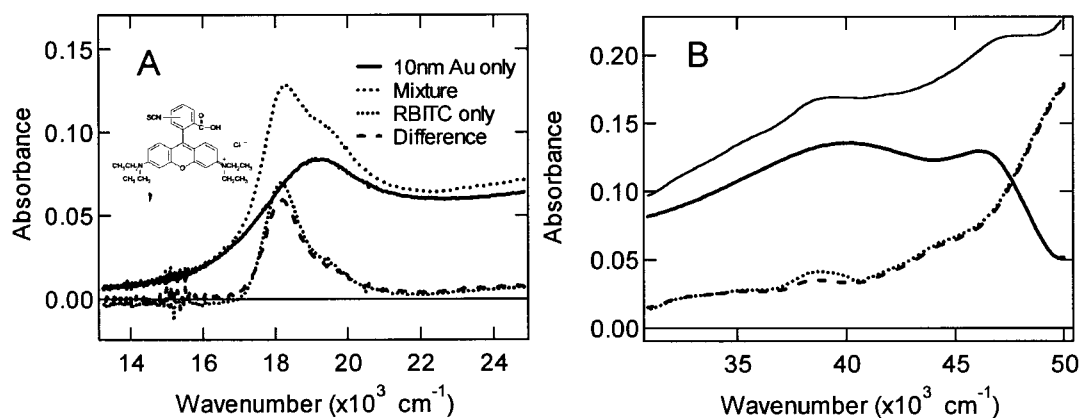

Figure 2. UV−vis spectrum of the class I adsorbate, RBITC (1.5×10^{-6} M), adsorbed to 10 nm mercaptooctanoate stabilized Au nanoparticles in a 50/50 H$_2$O/MeOH solvent. (A) The plasmon band of Au at $\omega_p \approx 19\,200$ cm^{-1} and the RBITC $\pi-\pi^*$ transition at 18 080 cm^{-1} are shown. (B) A broad band of the mercaptooctanoate stabilizer is observed at 39 840 cm^{-1} and a narrow band due to RBITC observed at 38 760 cm^{-1}. The nanoparticle absorption appears to have a second maximum at 46 080 cm^{-1} when mercaptooctanoate ligands are used as the capping ligand to stabilize the nanoparticle. There is a small decrease in the mercaptooctanoate absorption in the RBITC difference spectrum (---).

The surface area of the nanoparticles and each of the molecules was estimated to provide an initial target for the concentration necessary for complete monolayer coverage. However, titration of adsorbate molecules provided a more accurate estimate of the number of adsorbed molecules per nanoparticle. This number ranged from 500 to 2000 molecules per nanoparticle monomer, depending on the monomer size. The dye concentrations were thus chosen to be well below the aggregation limit of the system. As aggregation leads to a time-dependent broadening and shift[59] of the nanoparticle plasmon spectrum followed by precipitation, it could easily be distinguished from the more subtle changes due to the adsorption of dye on the nanoparticle. Subtle changes in the plasmon band due to the changing dielectric constant around the monomer resulting from adsorption are to be expected and indeed observed.[17,15,42,50]

Dilutions of stock solutions of adsorbate molecules were mixed in equal volumes of the nanoparticle solution. These mixtures were allowed to equilibrate in dark, refrigerated conditions for a minimum of 12 h to allow for complete adsorption. As a control, matching concentrations of the nanoparticle alone and adsorbate alone were prepared and treated under the same conditions at the same time. UV−vis spectra were taken before and after the 12-h incubation period or at regular time intervals to observe spectral changes as a function of time.

Samples were centrifuged at 14 000 rpm for 30 min to determine if adsorption had occurred during the absorption experiments. After centrifugation, 90% of the supernate was removed from each sample and the remaining pellet was resuspended with the appropriate solvent used in the experiment. Spectra were then obtained for both the supernate and the resuspended pellet. As a control, we also centrifuged the nanoparticle alone and adsorbate alone under the same conditions.

Results

The observed spectral changes of surface adsorbed molecules (referred to as adsorbates) can be divided into two classes. Table 1 lists the adsorbates and the range of nanoparticles studied. Class I adsorbates shown in Figures 1−3 can in principle chemisorb to the surface of the nanoparticle. Class II adsorbates shown in Figures 4 and 5 exhibit strongly reduced absorption intensity on gold and silver nanoparticles and are electrostatically bound. The figures are arranged in order of decreasing intensity of the adsorbate spectrum on the nanoparticle as seen in the difference spectra. Difference spectra were obtained by subtracting the nanoparticle-only spectrum from the adsorbate-nanoparticle mixture. In the difference spectra of the nanoparticle−adsorbate complexes there is an overall reduction in absorbance of the nanoparticle in the entire visible region. The intensity
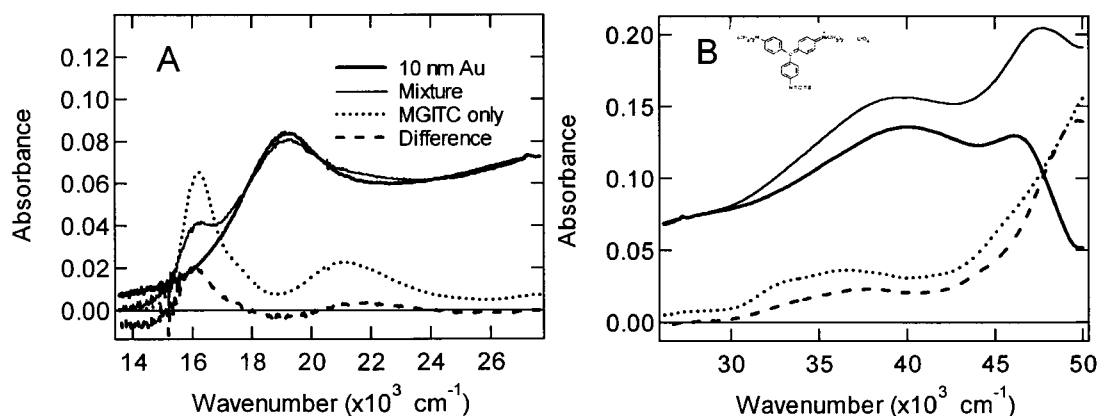
Figure 3. UV−vis spectrum of the adsorbate MGITC (9×10^{-7}M) adsorbed to 10 nm mercaptooctanoate stabilized Au nanoparticles in a 50/50 H_2O/MeOH solvent. Note that the spectrum of MGITC alone was acquired using pure MeOH as a solvent due to the partial lyophobicity of the MGITC solution. As the adsorption processes are identical, MeOH was chosen purely because it produces a less distorted MGITC spectrum. (A) The plasmon band of Au at $\omega_p \approx 19\,200$ cm^{-1} and the MGITC $\pi-\pi^*$ transition at 16 200 cm^{-1} are shown. (B) The bands of the mercaptooctanoate stabilizer observed at 39 840 cm^{-1} are reduced in intensity in the difference spectrum (---). Two bands due to MGITC observed at stabilizer are observed at 32 890 cm^{-1} and 35 840 cm^{-1}. There is also a reduction in intensity of the MGITC bands in the high wavenumber region.
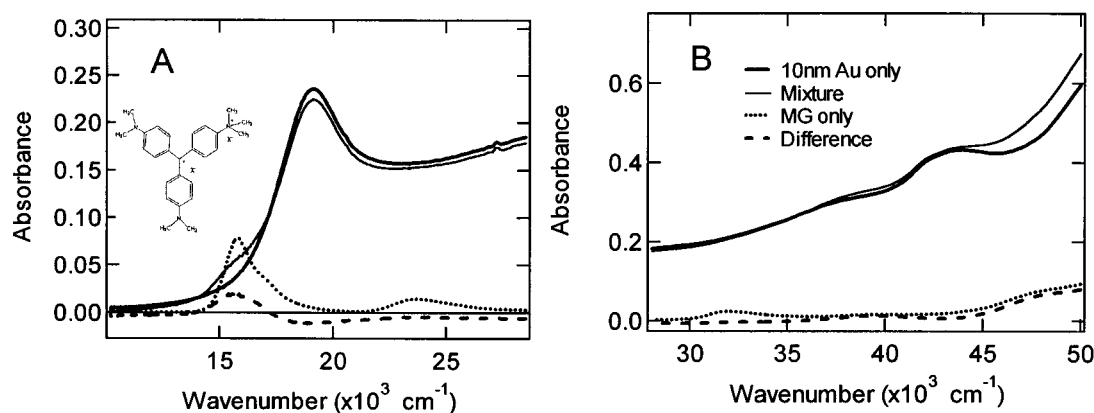

Figure 4. Illustration of class II adsorbate behavior. The UV−vis spectrum of MG (3×10^{-6} M) adsorbed to 10 nm BSPP stabilized Au nanoparticles in a 50/50 H_2O/MeOH solvent is shown. Note that the structure of MG is identical to that of MGITC except for the absence of an isothiocyano group in MG. (A) The plasmon band of Au and the $\pi-\pi^*$ MG bands are shown. (B) The bands due to the BSPP coating of the nanoparticle are seen at 43 800 cm^{-1}. The difference spectrum (---) shows relatively little change in the high wavenumber region.

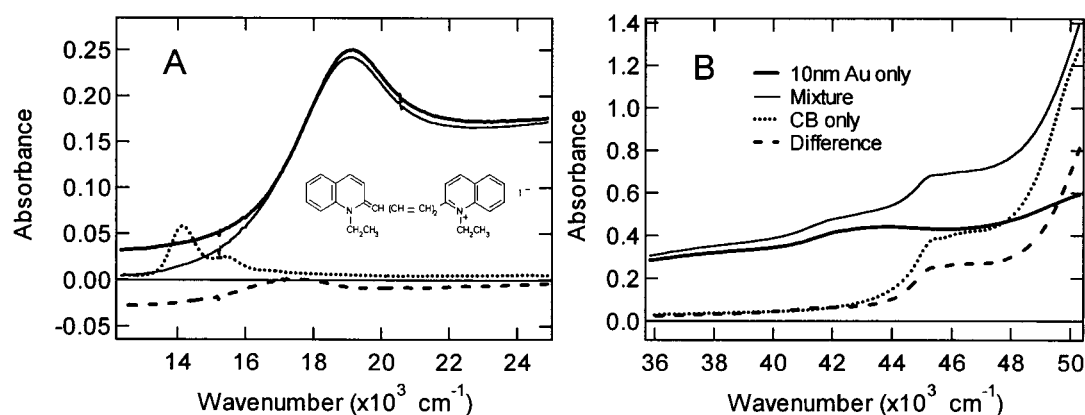**Figure 5.** UV−vis spectrum of a class II adsorbate, CB (4×10^{-7} M) adsorbed to 10 nm citrate stabilized Au nanoparticles in a 50/50 H_2O/MeOH solvent. The negative absorbance values may have originated from changes in reflectivity following adsorption of CB to the Au nanoparticles. (A) The plasmon band of Au and the $\pi-\pi^*$ CB bands are shown. (B) The bands due to the BSPP coating of the nanoparticle are seen at 43 800 cm^{-1}. The relative intensity of the CB band at 45 300 cm^{-1} is ≈0.65 in the difference spectrum (---) relative to free CB in solution at the same concentration (···).

order is also correlated with the energy of the lowest electronic transition as seen in Table 1. A baseline offset is evident in the difference spectra in all of the Figures except Figure 2. Centrifugation experiments further demonstrate that the spectral changes result from molecules adsorbed to a gold or silver nanoparticle. With the exception of pyridine, all of the adsor-

bates are precipitated along with all of the nanoparticles at the concentrations shown in Figures 1−5 by centrifugation at 14 000 rpm for several minutes.

The molecules can be divided into two classes called class I and class II based on the spectral features listed in Table 1. Class I adsorbates typically exhibit difference absorption spectra

(before and after mixing with a particular nanoparticle solution) that are as strong as the absorption spectrum of the dye alone. The spectra of these adsorbates are called "additive". For most of the adsorbates there is little or no change in the absorption intensity due to the electric field of surface plasmons. There is an enhancement in the absorption spectrum of F5ITC by a factor of 5 (data not shown); however, the latter effect is due to a solvatochromic shift caused by the surface charge of the nanoparticle. Class I adsorbates pyridine and RBITC adsorbed on 10 nm Au are shown in Figures 1 and 2, respectively. For these two molecules the spectra are nearly additive except for a baseline offset due to a reduction in scattering by the nanoparticles. Class I adsorbates all have lone pairs capable of interacting with metal surface in competition with the stabilizing ligands such as BSPP.[60] Molecules with isothiocyano (ITC) groups such as MGITC and RBITC can, in principle, compete with and displace citrate or BSPP on the surface of the nanoparticle.[61] It is possible that the dyes can displace citrate or BSPP due to interactions of the π-system of the molecule with the surface as well. There is no evidence that the ITC groups give rise to stronger binding than interaction of dyes that lack the ITC moiety. Pyridine has a weak interaction with Ag surfaces and may lie flat on the surface at low coverage.[62,63] Adsorbed pyridine has an additional feature; its system of π orbitals adjacent to the metal particle can interact strongly if it is bound in a geometry perpendicular to the surface. The example of pyridine shown in Figure 1 is particularly interesting, given that pyridine is the most studied molecule in the SERS literature. Raman scattering of surface adsorbed pyridine is known to be enhanced by a significant factor.[11,13,21,32,45,46] Despite this there is almost no discernible change in the pyridine band at 51 000 cm^{-1} (196 nm) or the vibronic band at 38 000 cm^{-1} (263 nm) shown in Figure 1B. Pyridine is somewhat anomalous in its weak interaction with nanoparticles. Neither pyridine nor the other class I adsorbates show any discernible enhancement in their absorption bands.

Centrifugation experiments show that the dyes shown in Figures 2−5 and in Table 1 are bound to nanoparticles. Figure 2 shows RBITC adsorbed to 10 nm mercaptooctanoate stabilized Au nanoparticles. The absorption spectrum for RBITC is additive to that of the nanoparticle. Similar results are obtained with BSPP and citrate stabilized 10 nm nanoparticles and with citrate stabilized 30 nm Ag and Au nanoparticles (see Table 1). Upon centrifugation, the spectrum of the supernate showed the amount of RBITC that remains in solution to be insignificant. When 10 nm nanoparticles shown in Figure 2 were resuspended, the shifted and broadened plasmon band in the precipitate spectrum provided evidence of aggregation (data not shown). Control experiments were performed by centrifugation of the adsorbate (RBITC) and the adsorbent (10 nm mercaptooctanoate stabilized Au) by themselves under identical solvent conditions. The RBITC-only control showed no change in the RBITC absorption spectrum following centrifugation, whereas the nanoparticle-only control showed 100% recovery of the precipitate as monomer nanoparticles after resuspension.

Figure 3 shows that the adsorbate MGITC has a reduction in absorption intensity in nanoparticle solutions. MGITC yielded similar results upon adsorption to 10 and 30 nm gold nanoparticles with all three stabilizers (see Table 1). MGITC is a significant choice since it has a structure similar to MG except that the trimethylamino group is replaced by an isothiocyano group, which allows for the possibility of chemisorption. However, the spectral differences are not great since both dyes show a decrease in absorption intensity in the difference spectra
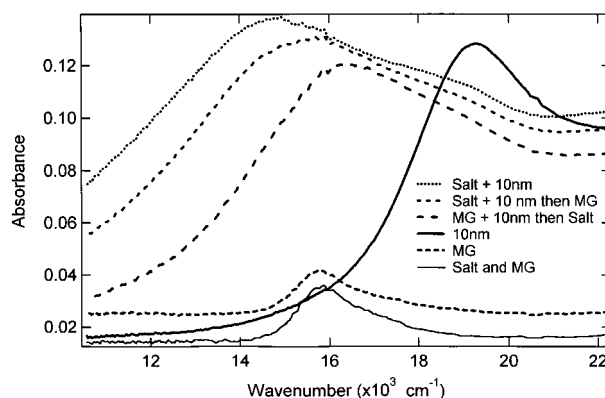

Figure 6. UV−vis spectrum of MG (1×10^{-6} M) adsorbed to 10 nm citrate stabilized Au nanoparticles in a 50/50 H$_2$O/MeOH solvent in the presence and absence of salt. The comparison is made between the monomer colloid ($\omega_p = 19\,100$ cm^{-1}) and the spectra of aggregated colloids in the presence of 100 mM NaCl (···) and two sample containing both MG dye and NaCl. The order of addition of MG and NaCl is compared with the same final concentration of both dye and salt. The aggregated colloid solution was prepared by addition of NaCl first and then MG (- - -) compared to the reverse order of MG first and then NaCl ($-\,-\,-$).

compared to the free dye at the same concentration. The reduction in intensity of MG is only slightly larger than that of MGITC. It is perhaps more significant that the wavenumber maximum of the MG (15 770 cm^{-1}) transition is 430 cm^{-1} lower than that of the MGITC (16 200 cm^{-1}) transition (Table 1).

Class II adsorbates are characterized as having absorption spectra that appear to bleach upon adsorption to nanoparticles. Included in this class are CB and ICG, which are both similar in structure to the pseudoisocyanine molecule used in single molecule SERS studies.[46] Class II adsorbates are all positively charged and are most likely bound to nanoparticles by electrostatic interactions, consistent with the observation that class II adsorbates induce aggregation of nanoparticles at lower concentrations than class I adsorbates. Figure 4 shows that the MG absorption band bleaches upon adsorption to the surface of 10 nm Au nanoparticle. The magnitude of the bleach increases with time, and this may be associated with the time required for MG to adsorb to the nanoparticle surface. The bleach of the absorption spectrum of MG shown in Figure 4 is observed after 18 h. Figure 5 shows a dramatic example of class II behavior. After centrifugation of samples of 1 μM MG adsorbed on the surface of a 0.2−1 nM suspension of 10 nm BSPP stabilized Au, no recovery of the MG absorption spectrum was observed. The absorption spectrum of another class II adsorbate, CB is completely absent in the adsorbate−nanoparticle difference spectrum. The centrifugation results for CB and all other class II adsorbates were similar to those for MG. The samples are quite stable at the concentration of adsorbate shown in Figures 1−5 and there was no sign of aggregation after two weeks of storage (data not shown). These observations confirm that the dye concentrations used are well below the aggregation limit. Experiments with class II dyes on 60 and 100 nm Au particles resulted in some bleaching of the absorption spectrum as well. However, colloidal suspensions of these larger nanoparticles began to aggregate prior to complete adsorption of the dye.

The observation of surface-enhanced Raman scattering in solution is usually induced by addition of salt. The role of the salt is to induce aggregation in the suspension of colloidal nanoparticles. Figure 6 shows the effect of adding 100 mM NaCl to a suspension of 10 nm Au particles. The shift of the plasmon band of the 10 nm Au particles to lower wavenumber and the

broadening are well-known indicators of nanoparticle aggregation. The point of Figure 6 is to compare the effect of adding both the MG dye and salt. The first observation is that the effect of adding salt is smaller when MG is present. The order of addition of the MG dye and salt is important, and a smaller effect is obtained when the MG dye is added first and then salt is added than for the reverse order. There is no obvious MG band in the aggregate spectrum shown in Figure 6. Once again absorption enhancement is conspicuously absent. Similar effects are obtained with three other dyes representing both classes I and II (CV, ICG, and RBITC) studied by the same method. For CV and RBITC there is a small residual band from the dye in the aggregate spectrum. In all cases the presence of the dye reduces the plasmon shift due to aggregation.

Discussion

The distinction between additive adsorbate spectra (class I) and bleaching of adsorbate spectra (class II) may arise from a number of possible effects. We consider (1) an apparent breakdown of Beer's law due to sample inhomogeneity, (2) saturation due to strong electromagnetic fields, (3) surface interactions, i.e., chemisorption versus physisorption, (4) surface selection rules due to differences in orientation, and (5) surface selection rule that is wavelength dependent due to the frequency dependent dielectric constant of gold. These effects may be interrelated since all of the adsorbates belonging to class I have either a lone pair or an isothiocyano group that would allow for a perpendicular orientation, as well as chemisorption to the surface. The adsorbates belonging to class II interact electrostatically (physisorption) with the passivating layer (citrate, BSPP, or mercaptooctanoate) of the nanoparticle, suggesting an orientation parallel to the surface. However, there are no observable differences that arise due to differences in the stabilizer in any of the molecules that have been investigated. Nor does it appear that the presence of an isocyanate group gives rise to a systematic difference. In other words, there is no clear evidence for an orientational effect between class I and II. Comparison of the adsorbates in Table 1 shows that the magnitude of ω_{max} of the adsorbate relative to the plasmon frequency, ω_p, appears to play an important role, and in fact, we suggest the dominant role. More precisely, the observed plasmon absorption transition is $\omega_{Fröhlich}$, which is related to the plasmon frequency ω_p by a geometrical factor. For a sphere $\omega_{Fröhlich} = \omega_p/\sqrt{3}$. For 10 nm Au nanoparticles $\omega_{Fröhlich}$ is the observed band at 19 200 cm^{-1} in Figures 1–5. In the following, we consider how the optical properties of a colloidal suspension of nanoparticles give rise to the observed results. Our basic model assumes that the dyes interact with the surface through either electrostatic binding or chemical displacement, but in either case the transition moment of the dye is largely parallel to the surface of the nanoparticle. This model gives rise to a simple interpretation based on the well-known surface selection rules on a conducting surface, with the caveat that the conductivity of the surface decreases to zero at the frequency of the maximum of the plasmon band.

In absorption spectroscopy it is often assumed that systems are optically homogeneous so that absorption spectra of individual components can be added linearly. Even if the particle size is smaller than the wavelength, a colloidal suspension may not always fulfill this requirement, particularly if it consists of metallic particles that interact very strongly with electromagnetic radiation. In that case the effective optical diameter of the particle may be a multiple of the actual diameter.[64] This implies

that, although adsorbed on the actual surface, one could consider the dye molecule to be well *inside* the particle, optically speaking. In the nonhomogeneous case one should consider the zone around the particles and the embedding solvent as two subsystems for which the resulting intensities should be added and then the logarithm taken, rather than simply adding the absorptions as in the homogeneous case. This may lead to an apparent violation of Beer's law. In the nonhomogeneous case the interaction of adsorbates with a colloidal particle could thus give rise to a masking effect of the adsorbate absorption spectrum. The effective optical particle size depends on the frequency and is particularly large just below $\omega_{Fröhlich}$, where the interaction of the metal with the electromagnetic wave is large. The plasmon frequency typically represents the frequency above which a metal begins to lose its ability to conduct. For molecular transitions with frequencies $\omega > \omega_{Fröhlich}$ the particle becomes transparent, the optical particle size will approach the actual one, and spectra are once again additive or more nearly so. Inhomogeneity of absorption is consistent with the data in Figures 1–5 since the values of ω_{max} of the respective molecules span the spectral region of the plasmon band, $\omega_{Fröhlich}$.

In the spectral region near $\omega_{Fröhlich}$ the surface selection rules are also predicted to change. The surface selection rules below $\omega_{Fröhlich}$ are those of a conductor. Using the Fresnel equations, the radiation at the surface is $E = E_i(1 - r)$ where $r = 1$ for a tangential polarization and $r = -1$ for a radial polarization and E_i is the incident electric field.[5] Below $\omega_{Fröhlich}$ the surface selection rules predict the well-known condition that the absorption of a molecule will vanish if its transition moment is parallel to a surface and will be enhanced by a factor of 2 if its transition moment is perpendicular to the surface. In the vicinity of $\omega_{Fröhlich}$ the surface selection rules become $E = E_i(1 - r)$, where $r = -1$ for tangential polarization and $r = 1$ for radial polarization. For molecules with transition moments parallel to the surface the absorption intensity of molecular electronic transitions will be reduced when $\omega_{max} < \omega_{Fröhlich}$ and progressively less affected as ω_{max} becomes larger than $\omega_{Fröhlich}$. This is roughly in agreement with the experimental observations; however, there is no proof that the molecules adsorb to the surface with their transition moments parallel to the surface. For molecules that bind with transition moments perpendicular to the surface, the absorption spectrum should be observed for $\omega_{max} < \omega_{Fröhlich}$ and vanish when $\omega_{max} \approx \omega_{Fröhlich}$.

If the surface field were extremely large, as suggested by theories of surface-enhanced Raman spectroscopy, it would be possible for bleaching to result from saturation of the electronic transition. If we consider the equality of the Einstein B coefficients for absorption and stimulated emission for a two-level system, it is theoretically possible to drive one-half of a population of molecules into the excited state. Under these conditions, for radiation density ρ the upward transition rate $B_{12}\rho$ and downward transition rate $B_{21}\rho$ are equal. This condition will be realized in the limit of very high radiation density. Saturation does not preclude Raman scattering, and thus, this mechanism is also consistent with the observation of SERS. We consider the order of magnitude of the electric field enhancement required for saturation to be a plausible explanation for the data observed in Figures 1–5. For a typical molecule of the type considered here with an extinction coefficient, $\epsilon \approx$ 10 000 M^{-1} cm^{-1} and a photon energy of $h\nu/c \approx 20\,000$ cm^{-1}, we can estimate that an intensity of approximately $I \approx 10^8$ W/cm^2 would be required to saturate the electronic transition. The optical pumping transition rate of $\sigma_A I/h\nu$, where $\sigma_A = 2303\epsilon/N_A$ (N_A is Avogadro's number), gives rise to an excitation

Optical Properties of Dye Molecules

J. Phys. Chem. A, Vol. 106, No. 28, 2002 **6539**

rate of 10^{10} s^{-1}. The rate is roughly 10 times greater than typical nonradiative deactivation pathways and would be sufficient to produce a significant excited-state population. The intensity at 20 000 cm^{-1} is approximately $I \approx 10^{-6}$ W/cm^2 in the photodiode array spectrometer. Given that the electric field is proportional to the square root of the intensity, the required enhancement of the electric field is $g \approx 10^7$ in order to achieve saturation under the conditions of the present study. The factor g in eq 5 has been reported to be as large as 10^3 in theoretical work; however, there is no theory that predicts an enhancement of 10^7 as required for saturation of the absorption transition. Saturation and thus the electromagnetic mechanism of enhancement cannot explain the observed disappearance of the molecular absorption of class II adsorbates.

The role of orientation is difficult to disentangle since the molecules that chemisorb will also tend to have a more perpendicular orientation with respect to the nanoparticle surface. The observation that the relative intensities of bands on a single molecule vary depending on the relationship of ω_{max} and $\omega_{Fröhlich}$ is most important for deciding between inhomogeneity and surface selection rules as the explanation for the data. Inspection of panels A and B in Figures 2−5 reveals that in every case the electronic transitions above the plasmon band have greater relative intensity than those below *even on the same molecule*. For example, the dye cyanine blue spectra shown in Figure 5 provide strong evidence for a mechanism for reduction of absorption intensity due to the relative change in particle conductivity above $\omega_{Fröhlich}$. CB has two electronic transitions with ω_{max} at 14 200 and 45 250 cm^{-1}, which are below and above $\omega_{Fröhlich}$, respectively. The former vanishes entirely (Figure 5A), while the latter is attenuated by a factor of 1.6 (Figure 5B) following adsorption onto a nanoparticle. Since both electronic transitions are on the same molecule, this suggests that a change in the interaction of electromagnetic radiation with the molecule arises from the change in surface reflectivity of the nanoparticle above the plasmon band. CB is electrostatically bound to the surface layer (citrate, BSPP or mercaptooctanoate) and its transition moment must be nearly parallel to the surface. In this case, the surface selection rules would indicate that no absorption intensity for CB should be observed below $\omega_{Fröhlich}$ and some intensity should be observed as the particle becomes nonconducting above $\omega_{Fröhlich}$. The correlation of transition energy relative to $\omega_{Fröhlich}$ with the observed absorption intensity is consistent with a role for surface selection rules. There are two further hypotheses that can be considered corresponding to the electromagnetic and chemical mechanisms for surface-enhanced Raman scattering, respectively. In the following we show that neither of these can explain the absorption data presented here.

In surface-enhanced Raman theory, a chemical mechanism of enhancement has been presented as an alternative to the electromagnetic mechanism. The chemical mechanism may arise from mixing of metal orbitals with orbitals on a molecule, providing charge transfer states that provide a resonant Raman mechanism at much lower energies than those available in the free molecule. Thus, the chemical mechanism could be a manifestation of resonance Raman enhancement. Such a mechanism could only hold for molecules that are bound to the surface, i.e., class I molecules. However, these molecules do not show any enhancement in their absorption spectra. Absorption bands at 19 720 and 18 620 cm^{-1}, such as those observed in 2 nm gold particles with adsorbed RBITC, are not observed in the larger colloids studied here.[65] Weak charge-transfer bands may be present in some of the spectra, but these are difficult to

distinguish from the background scattering offset in the difference spectra.

The effects that are observed on the absorption spectra appear to follow the surface selection rules expected for a gold surface if the dyes are adsorbed such that their π-systems are parallel to the surface of the nanoparticle. This occurs regardless of the nature of the interaction with the stabilizer. In a simple Drude model the dielectric constant of gold is $\epsilon = 1 - \omega_p^2/\omega^2 = 0$ at the plasmon frequency ($\omega = \omega_p$). The absorption cross section, σ_A, of the metal particle itself is proportional the square of $g = (\epsilon - \epsilon_o)/(\epsilon + 2\epsilon_o)$, as given above in eqs 1 and 5, respectively. At the Fröhlich frequency, the denominator approaches zero since $\epsilon = -2\epsilon_o$ and σ_A goes through a maximum.[64] Thus, in solution $|\epsilon| \approx -4.4$ at the Fröhlich frequency, but it becomes rapidly negative on the lower wavenumber side of the plasmon band ($\omega < \omega_{Fröhlich}$). The large negative dielectric constant implies that gold acts as a reflector to the red of the plasmon band. For molecules whose transition moments are parallel to the surface, there is a cancellation of the field and no spectral features will be observed for $\omega \ll \omega_{Fröhlich}$ in accordance with the surface selection rules.[5] The important observation here is that complete cancellation is observed at ≈ 700 nm (14 300 cm^{-1}), where $|\epsilon| \approx -16$ for bulk Au. On the other hand for $\omega \gg \omega_{Fröhlich}$ gold acts as an insulator. Thus, there is no surface cancellation of fields that interact with adsorbed dye molecules, and spectra are observed even for molecules that lie flat on the surface. The surface selection rules are predicted to change at the resonance condition so that the electric field does not cancel and a dye molecule with a transition moment parallel to the surface will be observed.[5] Hence, we see that molecular absorption spectra at or above $\omega_{Fröhlich}$ are not affected by the particle and are additive with the nanoparticle spectrum.

The above model for the electromagnetic mechanism for interaction of molecules with nanoparticles provides the simplest explanation for the observations in this study as well as being important for consideration of the mechanism of Raman scattering. The monomers studied here are small isolated nanoparticles that would not be expected to show enhancement via an electromagnetic mechanism. However, experiments carried out using particles of 30 nm and even 60 nm radius showed similar results, raising the issue of how these results bear on the observation of single molecule SERS. The real issue is to precisely define the term "single molecule" in a SERS experiment. The present study suggests that SERS on a single colloid is not likely to be observed. It is difficult to rationalize a SERS enhancement mechanism for a molecule whose absorption is bleached, no matter what the mechanism.

These observations are in agreement with a large body of data that suggest that SERS enhancement is small or absent for monomer colloids and is only observed when salt is added to induce aggregation.[37,43,44,66−68] However, the experiments shown in Figure 6 and other similar experiments indicate that there is no large increase in absorption cross section when salt is added to a metal colloid/dye suspension. The electromagnetic mechanism is likely to be important for larger more corrugated structures with length scales of the order of the excitation laser light (>500 nm). Although the enhancement of a single molecule on a large structure is possible,[69,44,70] the reduction in absorption intensity adsorbates such as CB presents conceptual problems for large Raman enhancements for any near-infrared dye.[71−74] In a suspension there are many phenomena that can give rise to observed spectral features. It is relevant to note that cyanine dyes show excitonic red shifts formation of J-aggregates[75−77] and large solvatochromism even in the absence of

nanoparticles. In fact, the presence of nanoparticles may result in a bleach of J-aggregate spectra.[78] The nature of extremely large electromagnetic enhancements reported in surface-enhanced Raman observations is still in need of further study.

Supporting Information Available: Structures for the dyes used in the study are given. This material is available free of charge via the Internet at http://pubs.acs.org.

References and Notes

(1) Moskovits, M. *Rev. Mod. Phys.* **1985**, *57*, 783−826.
(2) Tully, J. C. *Ann. Rev. Phys. Chem.* **2000**, *51*, 153−178.
(3) Weitz, D. A.; Garoff, S.; Gersten, J. I.; Nitzan, A. *J. Phys. Chem.* **1983**, *78*, 5324−5338.
(4) Philpott, M. R. *J. Chem. Phys.* **1975**, *62*, 1812−1817.
(5) Moskovits, M.; Suh, J. S. *J. Chem. Phys.* **1984**, *88*, 5526−5530.
(6) Creighton, J. A. *Surf. Sci.* **1983**, *124*, 209−219.
(7) Campion, A.; Kambhampati, P. *Chem. Soc. Rev.* **1998**, *27*, 241−250.
(8) Keller, O.; Liu, A.; Zayats, A. *Opt. Commun.* **1994**, *110*, 604−610.
(9) Voisin, C.; Fatti, N. D.; Christofilos, D.; Vallee, F. *J. Phys. Chem. B* **2001**, *105*, 2264−2280.
(10) Kerker, M. *Selected Papers on Surface-Enhanced Raman Scattering*; SPIE, The International Society for Optical Engineering: Bellingham, MA, 1990; Vol. MS 10.
(11) Pan, D.; Philips, D. L. *Chem. Phys. Lett.* **1997**, *275*, 227−233.
(12) Kurokawa, Y.; Imai, Y.; Tamai, Y. *Analyst* **1997**, *122*, 941−944.
(13) Zeisel, D.; Deckert, V.; Zenobi, R.; Vo-Dinh, T. *Chem. Phys. Lett.* **1998**, *283*, 381−385.
(14) DiLella, D. P.; Gohin, A.; Lipson, R. H.; McBreen, P.; Moskovits, M. *J. Chem. Phys.* **1980**, *73*, 4282−4295.
(15) Moskovits, M.; McBreen, P. *J. Chem. Phys.* **1978**, *68*, 4992−5000.
(16) Cai, W.; Wan, L.; Noda, H.; Hibino, Y.; Ataka, K.; Osawa, M. *Langmuir* **1998**, *14*, 6992−6998.
(17) Garoff, S.; Weitz, D. A.; Gramila, T. J.; Hanson, C. D. *Opt. Lett.* **1981**, *6*, 245−247.
(18) Greenler, R. G. *J. Chem. Phys*. **1965**, *44*, 310−315.
(19) Zhang, Z.; Imae, T. *J. Colloid Interface Sci.* **2001**, *233*, 99−106.
(20) Zhang, Z.; Imae, T. *J. Colloid Interface Sci.* **2001**, *233*, 107−111.
(21) Fleischmann, M.; Hendra, P. J.; McQuillan, A. J. *Chem. Phys. Lett.* **1974**, *26*, 163−166.
(22) Clark, H. A.; Campagnola, P. J.; Wuskell, J. P.; Lewis, A.; Loew, L. M. *J. Am. Chem. Soc.* **2000**, *122*, 10234−10235.
(23) Small, J. R.; Foster, N. S.; Amonette, J. E.; Autrey, T. *Appl. Spectrosc.* **2000**, *54*, 1142−1150.
(24) Lettinga, M. P.; Zuilhof, H.; Zandvoort, M. A. M. J. v. *Phys. Chem. Chem. Phys* **2000**, *2*, 3697−3707.
(25) Makarova, O. V.; Ostafin, A. E.; Miyoshi, H.; J R Norris, J. *J. Phys. Chem. B* **1999**, *105*, 9080−9084.
(26) Ahmadi, T. S.; Lognov, S. L.; El-Sayed, M. A. *J. Phys. Chem.* **1996**, *100*, 8053−8056.
(27) Chun-ping, Z.; Feng-qi, Y.; Guang-yin, Z. *J. Raman. Spectrosc.* **1989**, *20*, 431−434.
(28) Prochazka, M.; Hanzlikova, J.; Stepanek, J.; Baumruk, V. *J. Mol. Struct.* **1997**, *410−411*, 77−79.
(29) Sbrana, G.; Neto, N.; Muniz-Miranda, M.; Nicentini, M. *J. Phys. Chem.* **1990**, *94*, 3706−3710.
(30) Kim, M.; Itol, K. *J. Phys. Chem.* **1987**, *91*, 126−131.
(31) Vlckova, B.; Matejka, P.; Simonova, J.; Cermakova, K.; Pancoska, P.; Baumruk, V. *J. Phys. Chem.* **1993**, *97*, 9719−9729.
(32) Marchi, M. C.; Blimes, S. A.; Blimes, G. M. *J. Colloid Interface Sci.* **1999**, *218*, 112−117.
(33) Weitz, D. A.; Lin, M. Y.; Sandroff, C. J. *Surf. Sci.* **1985**, *158*, 147−164.
(34) Ahera, A. M.; Garrell, R. L. *Anal. Chem.* **1987**, *59*, 2813−2816.
(35) Herne, T. M.; Garrell, R. L. *Anal. Chem.* **1991**, *62*, 2290−2294.
(36) Neddersen, J.; Chumanov, G.; Cotton, T. M. *Appl. Spectrosc* **1993**, *47*, 1993.
(37) Srnova, I.; Prochazka, M.; Vlckova, B.; Stepanek, J.; Maly, P. *Langmuir* **1998**, *14*, 4666−4670.
(38) Prochazka, M.; Mojzes, P.; Stepanek, J.; Vlckova, B.; Turpin, P. *Anal. Chem.* **1997**, *69*, 5103−5108.
(39) Templeton, A. C.; Wuelfing, W. P.; Murray, R. W. *Acc. Chem. Res.* **2000**, *33*, 27−36.

(40) Kang, S. Y.; Jeon, I. C.; Kim, K. *Appl. Spectrosc.* **1998**, *52*, 278−283.
(41) Litorja, M.; Haynes, C. L.; Haes, A. J.; Jensen, T. R.; Duyne, R. P. V. *J. Phys. Chem. B* **2001**, *105*, 6907−6915.
(42) Kerker, M. *J. Colloid Interface Sci.* **1985**, *105*, 297−314.
(43) Song, O. K.; Pauley, M. A.; Wang, C. H.; Jen, A. K. Y. *J. Raman. Spectrosc.* **1996**, *27*, 685−690.
(44) Michaels, A. M.; Jiang, J.; Brus, L. *J. Phys. Chem. B* **2000**, *104*, 11965−11971.
(45) Michaels, A. M.; Nirmal, N.; Brus, L. E. *J. Am. Chem. Soc.* **1999**, *121*, 9932−9939.
(46) Kneipp, K.; Kneipp, H.; Deinum, G.; Itzkan, I.; Dasari, R. R.; Feld, M. S. *Appl. Spectrosc.* **1998**, *52*, 175−178.
(47) *Biological Applications of Raman Spectroscopy*; Myers, A. B., Mathies, R. A., Eds.; Wiley: New York, 1988; Vol. 1.
(48) Templeton, A. C.; Pietron, J. J.; Murray, R. W.; Mulvaney, P. *J. Phys. Chem. B* **2000**, *104*, 564−570.
(49) Fowles, G. R. *Introduction to Modern Optics*, 2nd ed.; Holt, Rinehart and Winston: New York, 1975.
(50) Craighead, H. G.; Glass, A. M. *Opt. Lett.* **1981**, *6*, 248−250.
(51) Thomas, K. G.; Kamat, P. V. *J. Am. Chem. Soc.* **2000**, *122*, 2655−2656.
(52) Aravind, P. K.; Nitzan, A.; Metiu, H. *Surf. Sci.* **1981**, *110*, 189−204.
(53) Osawa, M.; Ikeda, M. *J. Phys. Chem.* **1991**, *95*, 9914−9919.
(54) Jensen, T. R.; Duyne, R. P. V.; Johnson, S. A.; Maroni, V. A. *Appl. Spectrosc.* **2000**, *54*, 371−377.
(55) Schatz, G. C. *J. Mol. Struct.* (*THEOCHEM*) **2001**, *573*, 73−80.
(56) Malinsky, M. D.; Kelly, K. L.; Schatz, G. C.; Duyne, R. P. V. *J. Phys. Chem. B* **2001**, *105*, 2343−2350.
(57) Jensen, T. R.; Duval, M. L.; Kelly, K. L.; Lazarides, A. A.; Schatz, G. C.; Duyne, R. P. V. *J. Phys. Chem. B* **1999**, *103*, 9846−9853.
(58) Mohamed, M. B.; Volkov, V.; Link, S.; El-Sayed, M. A. *Chem. Phys. Lett.* **2000**, *317*, 517−523.
(59) Storhoff, J. J.; Lazarides, A. A.; Mucic, R. C.; Mirkin, C. A.; Letsinger, R. L.; Schatz, G. C. *J. Am. Chem. Soc.* **2000**, *122*, 4640−4650.
(60) Puddephatt, R. J. In *Comprehensive Coordination Chemistry*; Wilkinson, G., Gillard, R. D., McCleverty, J. A., Eds.; Pergamon Press: Oxford, 1987; Vol. 5, pp 862−91.
(61) Dawson, A.; Kamat, P. V. *J. Phys. Chem. B* **2000**, *104*, 11842−11846.
(62) Barradas, R. G.; Conway, B. E. *J. Electroanal. Chem.* **1963**, *6*, 314.
(63) Mohilner, D. M. In *Electroanalytical Chemistry*; Bard, A. J., Ed.; Marcel Dekker: New York, 1966; Vol. 1, p 355.
(64) Bohren, C. F.; Huffman, D. R. *Absorption and Scattering of Light by Small Particles*; John Wiley & Sons: New York, 1983.
(65) Chandrasekharan, N.; Kamat, P. V.; Hu, J.; Jones, G., II. *J. Phys. Chem. B* **2000**, *104*, 10000−10000.
(66) Lecomte, S.; Moreau, N. J.; Manfait, M.; Aubard, J.; Baron, M. H. *Biospectroscopy* **1995**, *1*, 423−436.
(67) Picorel, R.; Chumanov, G.; Cotton, T. M.; Montoya, G.; Toon, S.; Seibert, M. *J. Phys. Chem.* **1994**, *98*, 6017−6022.
(68) Jensen, T.; Kelly, L.; Lazarides, A.; Schatz, G. C. *J. Cluster Sci.* **1999**, *10*, 295−317.
(69) Xu, H. X.; Bjerneld, E. J.; Kall, M.; Borjesson, L. *Phys. Rev. Lett.* **1999**, *83*, 4357−4360.
(70) Xu, H. X.; Aizpurua, J.; Kall, M.; Apell, P. *Phys. Rev. E* **2000**, *62*, 4318−4324.
(71) Kneipp, K.; Kneipp, H.; Itzkan, I.; Dasari, R. R.; Feld, M. S. *Chem. Phys.* **1999**, *247*, 155−162.
(72) Maruyama, Y.; Ishikawa, M.; Futamata, M. *Chem. Lett.* **2001**, *8*, 834−835.
(73) Eggeling, C.; Schaffer, J.; Seidel, C. A. M.; Korte, J.; Brehm, G.; Schneider, S.; Schrof, W. *J. Phys. Chem. A* **2001**, *105*, 3673−3679.
(74) Krug, J. T.; Wang, G. D.; Emory, S. R.; Nie, S. M. *J. Am. Chem. Soc.* **1999**, *121*, 9208−9214.
(75) Jones, R. M.; Lu, L. D.; Helgeson, R.; Bergstedt, T. S.; McBranch, D. W.; Whitten, D. G. *Proc. Natl. Acad. Sci. U.S.A.* **2001**, *98*, 14769−14772.
(76) Chowdhury, A.; Wachsmann-Hogiu, S.; Bangal, P. R.; Raheem, I.; Peteanu, L. A. *J. Phys. Chem. B* **2001**, *105*, 12196−12201.
(77) von Berlepsch, H.; Bottcher, C.; Dahne, L. *J. Phys. Chem. B* **2000**, *104*, 8792−8799.
(78) Sato, T.; Tsugawa, F.; Tomita, T.; Kawasaki, M. *Chem. Lett.* **2001**, *5*, 402−403.